

**Fig. 5.** Model showing proposed mechanism by which CRSP and ARC-L regulate transcription. In this model, activators play a dual role in transcriptional activation. First, they recruit the CRSP coactivator to the promoter. Second, they induce conformational changes in the CRSP complex, which may facilitate transcription initiation by recruiting/stabilizing other cofactors and components of the preinitiation complex, including RNA polymerase II. Certain CRSP interactions may be activator-specific. However, upon binding additional ARC-L subunits (which may occur on activator-bound CRSP following multiple rounds of activated transcription), CRSP undergoes a structural change that may also result in dissociation of CRSP70. Now converted to ARC-L, coactivator function is lost and activated transcription is inhibited. The location of ARC-L-specific polypeptides (red) is based upon analysis detailed in Fig. 3D. The orientations of the complexes at the promoter are speculative. VP16 is shown in quotation marks because it does not directly bind DNA.

mere presence of the activation domain because of its small size (about 6% of the total mass) relative to the CRSP complex. Further, we have mapped the VP16 and SREBP-1a binding sites to comparatively small and distinct regions on the CRSP complex. This provides direct evidence that only a limited number (one or perhaps two) of CRSP subunits are targeted by a particular activator. Because VP16-CRSP and SREBP-CRSP are conformationally distinct in regions distal to the activator binding sites, we suggest that activator binding may induce long-range conformational changes. Thus, different protein surfaces in CRSP are likely exposed as a consequence of activator binding.

The conformational flexibility of the CRSP coactivator may have important implications for its mechanism of action. CRSP and its related coactivator complexes appear to be generally required for transcription and are targeted by a diverse array of regulatory proteins (22). Interestingly, different transcription activators can target different subunits of the CRSP complex (3, 9, 20, 21). Thus, despite binding the same coactivator complex, regulatory proteins may impart promoter-specific functions that may be dependent on CRSP conformation. For example, specific activator-induced CRSP conformations may regulate binding and recruitment of additional activators or cofactors to the preinitiation complex (Fig. 5). Furthermore, these conformational changes may trigger other (as yet undiscovered) enzymatic activities within the CRSP coactivator. Indeed, adopting a number of activator-dependent conformations may enable CRSP to perform

more specialized roles in transcriptional activation. Elucidation of these roles will be an important subject of future work.

**References and Notes**

1. R. E. Kingston, G. J. Narlikar, *Genes Dev.* **13**, 2339 (1999).
2. B. D. Lemon, R. Tjian, *Genes Dev.* **14**, 2551 (2000).
3. T. G. Boyer, M. E. D. Martin, E. Lees, R. P. Riccardi, A. J. Berk, *Nature* **399**, 276 (1999).

4. J. D. Fondell, H. Ge, R. G. Roeder, *Proc. Natl. Acad. Sci. U.S.A.* **93**, 8329 (1996).
5. W. Gu *et al.*, *Mol. Cell* **3**, 97 (1999).
6. Y. Kim, S. Bjorklund, Y. Li, M. H. Sayre, R. D. Kornberg, *Cell* **77**, 599 (1994).
7. S. Malik, W. Gu, W. Wu, J. Qin, R. G. Roeder, *Mol. Cell* **5**, 753 (2000).
8. A. M. Näär *et al.*, *Nature* **398**, 828 (1999).
9. C. Rachez *et al.*, *Nature* **398**, 824 (1999).
10. S. Ryu, S. Zhou, A. G. Ladurner, R. Tjian, *Nature* **397**, 446 (1999).
11. X. Sun *et al.*, *Mol. Cell* **2**, 213 (1998).
12. D. J. Taatjes, A. M. Näär, R. Tjian, data not shown.
13. A. M. Näär *et al.*, *Genes Dev.* **12**, 3020 (1998).
14. R. T. Kamakaka, M. Bulger, J. T. Kadonaga, *Genes Dev.* **7**, 1779 (1993).
15. Supplementary data is available at Science Online at [www.sciencemag.org/cgi/content/full/295/5557/1058/DC1](http://www.sciencemag.org/cgi/content/full/295/5557/1058/DC1)
16. The P1M fraction from a stable 293T human kidney cell line expressing Flag-tagged CRSP70 was used for CRSP purification via an anti-Flag affinity resin.
17. M. R. Dotson *et al.*, *Proc. Natl. Acad. Sci. U.S.A.* **97**, 14307 (2000).
18. S. Akoulitchev, S. Chuikov, D. Reinberg, *Nature* **407**, 102 (2000).
19. V. Booth, C. M. Koth, A. M. Edwards, C. H. Arrow-smith, *J. Biol. Chem.* **275**, 31266 (2000).
20. M. Ito *et al.*, *Mol. Cell* **3**, 361 (1999).
21. A. M. Näär, unpublished results.
22. C. Rachez, L. P. Freedman, *Curr. Opin. Cell Biol.* **13**, 274 (2001).
23. We thank J. Berger, J. Doudna, R. Freiman, A. Ladurner, B. Lemon, R. Losick, M. Marr, D. Rio, K. Shelton, and K. Yamamoto for critical reading of the manuscript. We also thank A. Ladurner and S. Ryu for the flag-70 cell line; A. Ladurner, S. Ryu, and W. Zhai for antibodies against CRSP70; Y. Nedialkov and S. Triezenberg for monoclonal antibodies against GST; and O. Fedin for scanning micrographs. D.J.T. is supported by a grant from the American Cancer Society (#PF0007801GMC). This work was funded by grants from the NIH and Howard Hughes Medical Institute.

9 August 2001; accepted 7 December 2001

## Linking Breeding and Wintering Ranges of a Migratory Songbird Using Stable Isotopes

D. R. Rubenstein,<sup>1,2\*†</sup> C. P. Chamberlain,<sup>2‡</sup> R. T. Holmes,<sup>1</sup> M. P. Ayres,<sup>1</sup> J. R. Waldbauer,<sup>2‡</sup> G. R. Graves,<sup>3</sup> N. C. Tuross<sup>4</sup>

We used the natural abundance of stable isotopes (carbon and hydrogen) in the feathers of a neotropical migrant songbird to determine where birds from particular breeding areas spend the winter and the extent to which breeding populations mix in winter quarters. We show that most birds wintering on western Caribbean islands come from the northern portion of the species' North American breeding range, whereas those on more easterly islands are primarily from southern breeding areas. Although segregated by breeding latitude, birds within local wintering areas derive from a wide range of breeding longitudes, indicating considerable population mixing with respect to breeding longitude. These results are useful for assessing the effects of wintering habitat loss on breeding population abundances and for predicting whether the demographic consequences will be concentrated or diffuse.

In recent decades, many species of neotropical migrant birds have shown marked changes in abundance—both increases and de-

creases—in parts of their North American breeding range (1, 2). These changes may be due to events occurring in the breeding

## REPORTS

grounds, in the wintering grounds, or during migration (3). Because these birds migrate long distances and are not easy to track year-round, it is difficult to determine at which points in the annual cycle their populations are most vulnerable (3). It is thus necessary to develop methods for differentiating among populations, for determining where birds from particular parts of the breeding range spend the winter, and for estimating the degree to which individuals from different breeding areas mix with individuals from other breeding areas in their wintering quarters (4, 5).

Determining how birds mix on the wintering grounds will be particularly important for understanding how wintering habitat loss could

affect abundances of breeding birds (4). Stable isotopes can be used to examine such potential links between the breeding and wintering ranges of migratory species (6–11). We used carbon and hydrogen isotopic ratios in the feathers of a neotropical migrant bird species to identify where individuals in particular wintering locations breed (breeding origins) and to assess whether individuals from different breeding areas co-occur in local wintering sites (population mixing). We described the isotopic patterns in feathers collected from almost 700 black-throated blue warblers (*Dendroica caerulescens*) throughout the species' breeding range in temperate North America and its main wintering range in the Greater Antilles (Fig. 1) (12). We then used the breeding ground isotopic patterns to build models from which we infer connections between the breeding and wintering ranges of this long-distance migrant.

In birds, the isotopic ratios of carbon and hydrogen (the nonexchangeable portion) are fixed permanently into inert keratin tissues such as feathers, and they reflect a bird's diet and the local environment in which it grew those tissues (13). For insectivorous birds such as the black-throated blue warbler, isotopic ratios in feathers reflect those of the insects they eat, which in turn reflect those of the plants on which the insects have fed (14). The isotopic ratios are fixed in the feathers at the time of molt, which for many migratory passerines, including the black-throated blue warbler, occurs in late summer on or near breeding locations (12). Because isotopic ratios show natural patterns of geographic vari-

ation (15), they provide useful markers for identifying breeding localities and, ultimately, for determining links between breeding and wintering sites (6).

Carbon and hydrogen isotopic ratios (expressed as  $\delta^{13}\text{C}$  and  $\delta\text{D}$  values, respectively) in black-throated blue warbler feathers vary systematically along a latitudinal gradient throughout the species' breeding range in temperate North America (6, 15). We determined the  $\delta^{13}\text{C}$  and  $\delta\text{D}$  values (16) of feathers collected from black-throated blue warblers (17) at 10 sites that span the species' breeding range in temperate North America, as well as at 11 sites on four islands across the species' wintering range in the Greater Antilles (Fig. 1) (18).  $\delta^{13}\text{C}$  and  $\delta\text{D}$  values in black-throated blue warbler feathers decrease with increasing breeding latitude in the temperate North American breeding grounds (Fig. 2, A and B) (19). In the Greater Antillean wintering grounds, isotopic ratios in black-throated blue warbler feathers also show a strong geographic pattern, with  $\delta^{13}\text{C}$  and  $\delta\text{D}$  values in feathers decreasing from Puerto Rico to Cuba (Fig. 2, C and D). Thus,  $\delta^{13}\text{C}$  and  $\delta\text{D}$  values decrease from east to west—that is, with increasing longitude—within the wintering range of this species.

We used these geographic patterns in breeding ground isotopic signatures to develop a regression model that predicts breeding latitude (breeding origins) of wintering warblers based on  $\delta^{13}\text{C}$  and  $\delta\text{D}$  values in their feathers (20). Results indicate that more birds from the northern portion of the breeding

<sup>1</sup>Department of Biological Sciences, <sup>2</sup>Department of Earth Sciences, Dartmouth College, Hanover, NH 03755, USA. <sup>3</sup>Department of Systematic Biology, <sup>4</sup>National Museum of Natural History, Smithsonian Institution, Washington, DC 20560, USA.

\*Present address: Department of Neurobiology and Behavior, Cornell University, Ithaca, NY 14853, USA.

†To whom correspondence should be addressed. E-mail: drr24@cornell.edu

‡Present address: Department of Geological and Environmental Sciences, Stanford University, Stanford, CA 94305, USA.

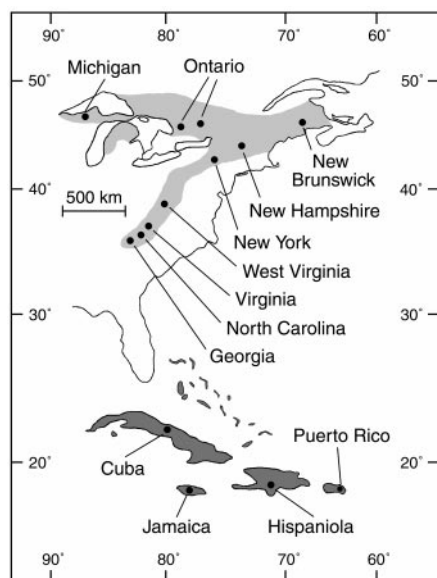
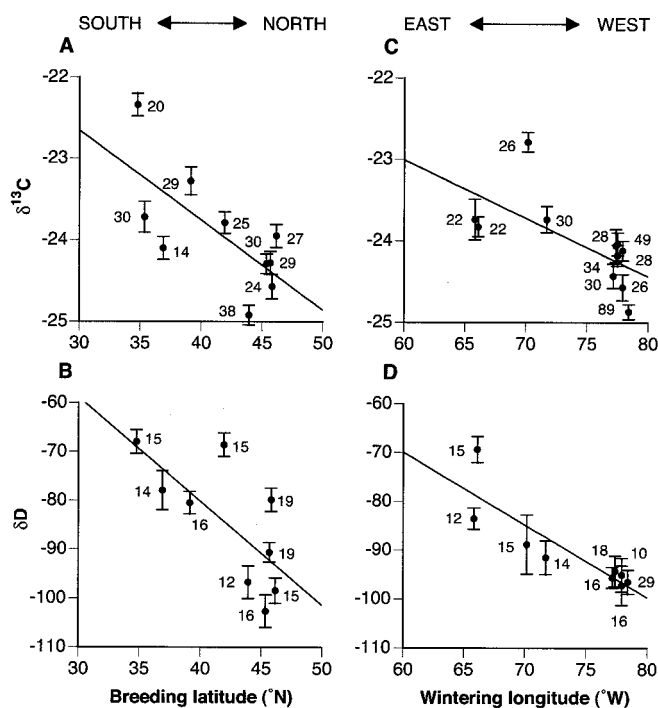


**Fig. 1.** Temperate North American breeding range and Greater Antillean wintering range of the black-throated blue warbler. A few individuals also winter in the Florida everglades, on the coast of the Yucatan Peninsula, and in Belize (12). Sampling locations in the breeding grounds and wintering grounds are indicated by black circles. In the Greater Antilles, samples were collected from individuals wintering in Jamaica (six sites in central and western portions), in Cuba (one site on a small cay, Cayo Coco, 15 km off the north-central coast), in Hispaniola (two sites in the Dominican Republic near the border with Haiti), and in Puerto Rico (three sites near the eastern end).

**Fig. 2.** Population means ( $\pm$ SE) of  $\delta^{13}\text{C}$  and  $\delta\text{D}$  in black-throated blue warbler feathers at different breeding latitudes and wintering longitudes. Sample sizes are indicated next to each site. (A)  $\delta^{13}\text{C}$  values from the temperate North America breeding range decrease with increasing breeding latitude [ $F_{1,8} = 7.67$ ,  $P = 0.024$ ,  $r^2 = 0.49$ , latitude =  $-19.35 - 0.11(\delta^{13}\text{C})$ ]. (B)  $\delta\text{D}$  values from the temperate North America breeding range decrease with increasing breeding latitude [ $F_{1,7} = 7.17$ ,  $P = 0.032$ ,  $r^2 = 0.51$ , latitude =  $1.32 - 2.02(\delta\text{D})$ ]. (C)  $\delta^{13}\text{C}$  values from the Greater Antillean wintering range decrease with increasing wintering longitude [ $F_{1,9} = 6.07$ ,  $P = 0.036$ ,  $r^2 = 0.40$ , longitude =  $-18.81 - 0.07(\delta^{13}\text{C})$ ]. (D)  $\delta\text{D}$  values from the Greater Antillean wintering range decrease with increasing wintering longitude [ $F_{1,7} = 22.93$ ,  $P = 0.002$ ,  $r^2 = 0.77$ , longitude =  $20.82 - 1.51(\delta\text{D})$ ].



range winter on the westerly islands of Cuba and Jamaica, whereas more birds from the southern portion of the breeding range winter on the easterly islands of Hispaniola and Puerto Rico (Fig. 3, A and B). Thus, black-throated blue warblers appear to segregate on the wintering grounds with respect to breeding latitude.

We developed a second model (21) that relates breeding longitude to isotopic ratios in the feathers of birds collected from the four most northerly breeding populations, which span ~26° of longitude (Fig. 1). We then used this model to estimate the range of

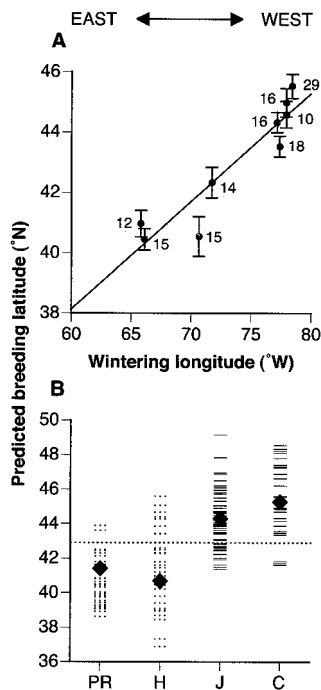


**Fig. 3.** Breeding latitudes of wintering black-throated blue warblers predicted from a regression model (20). (A) Population mean ( $\pm$ SE) predicted breeding latitudes from birds sampled at different wintering longitudes in the Greater Antilles (Fig. 1). Sample sizes are indicated next to each site. Predicted breeding latitude increases with increasing wintering longitude ( $F_{1,7} = 47.99$ ,  $P = 0.0002$ ,  $r^2 = 0.87$ ). (B) Predicted breeding latitudes of individuals sampled on islands in the western wintering range (solid horizontal lines) and on islands in the eastern wintering range (dotted horizontal lines) (C, Cuba; J, Jamaica; H, Hispaniola; PR, Puerto Rico). The dashed line divides the northern and southern portions of breeding range at 42.9°N, the midway point between the northernmost sampling location in the southern portion and the southernmost sampling location in the northern portion (Fig. 1). Diamonds indicate the mean predicted breeding latitudes for each island. A greater proportion of birds from the northern portion of the breeding range winter on the more westerly islands, whereas a greater proportion of birds from the southern portion of the breeding range winter on the more easterly islands ( $\chi^2 = 58.44$ ,  $df = 1$ ,  $n = 144$ ,  $P < 0.0001$ ).

breeding longitude values represented in feathers collected from local wintering sites. We constrained our analysis to only those feather samples from wintering birds that had previously been identified as coming from the northern portion of the breeding range (Fig. 3) (20) and to those wintering sites (four on the westerly islands) with sample sizes of  $\geq 10$  individuals. The predicted breeding longitudes of these wintering birds ranged from 65.9° to 82.5°W at Cayo Coco, Cuba ( $n = 25$ ); from 70.1° to 87.1°W at Baronhall Estates, Jamaica ( $n = 10$ ); from 69.3° to 89.8°W at Font Hill Nature Preserve, Jamaica ( $n = 15$ ); and from 73.5° to 85.0°W at Portland Ridge, Jamaica ( $n = 13$ ). Thus, individuals wintering at these four sites came from breeding areas spanning an average of 16.4° of longitude, or 63% of the ~26° of longitude over which this species breeds in temperate North America (Fig. 1). The predicted latitudinal range for these same individuals was 4.6°, or 27% of the ~17° of latitude over which this species breeds (Fig. 1). Thus, black-throated blue warblers in local wintering sites are well mixed with respect to breeding longitude, even though they tend to be segregated with respect to breeding latitude. Because the southern portion of the breeding range covers only a narrow longitudinal range, it was not possible to do a comparable analysis for birds wintering on the easterly islands.

Studies of other migratory songbird species have found morphological (22) and behavioral (23) evidence for segregation on the wintering grounds by breeding region, as well as morphological (24) and isotopic (10) evidence suggesting mixing of breeding populations at wintering sites. Our results from a single species sampled across its entire breeding and wintering ranges illustrate that wintering populations can be segregated with respect to one axis of their breeding distribution (latitude) even while they are mixed with respect to another (breeding longitude). Future research must determine whether other migratory species exhibit similar regional patterns of segregation on the wintering grounds, and whether their wintering populations also tend to be mixed differentially with respect to breeding latitude and longitude.

Understanding patterns of migration has important implications for the conservation of songbirds and other migratory species. Because black-throated blue warblers appear to segregate by breeding latitude on the wintering grounds, the changes in breeding abundance (2) could, in part, be a consequence of the variable rates and geographic scope of habitat loss incurred on the different Greater Antillean islands. According to our results, habitat loss in Cuba or Jamaica should have had diffuse effects on our study species' abundance throughout the northern portion of its breeding range,

but similar loss in Hispaniola or Puerto Rico should have had more concentrated and visible effects on abundances in the relatively narrow southern portion. In fact, breeding bird survey data from the past 30 years indicate declines in black-throated blue warbler abundance in the southern breeding areas—particularly at the southernmost extreme—and little change, or even increases, in abundance throughout much of the northern breeding range (2). Furthermore, the most extensive deforestation in the Greater Antilles (>97% of forestland) has occurred in Haiti (25), which lies on the island of Hispaniola. Our results connecting a high proportion of birds from the southernmost portion of the breeding range to the island of Hispaniola suggest a possible correlation between this severe wintering habitat loss and the sharpest breeding population declines. Understanding such geographic links between the breeding and wintering ranges and ultimately their relation to demographic trends is necessary to develop satisfactory models of songbird population dynamics (5). Only by considering events throughout the entire annual cycle can well-informed decisions be made about how best to conserve and manage declining populations of migratory birds.

**References and Notes**

1. F. C. James, C. E. McCulloch, D. A. Wiedenfeld, *Ecol. Appl.* **77**, 13 (1996).
2. J. R. Sauer, J. E. Hines, J. Fallon, *The North American Breeding Bird Survey, Results and Analysis 1966–2000. Version 2001.2* (U.S. Geological Survey Patuxent Wildlife Research Center, Laurel, MD, 2001).
3. T. W. Sherry, R. T. Holmes, in *Ecology and Management of Neotropical Migratory Birds: A Synthesis and Review of Critical Issues*, T. E. Martin, D. M. Finch, Eds. (Oxford Univ. Press, Oxford, 1995), pp. 85–120.
4. D. S. Wilcove, J. W. Terborgh, *Am. Birds* **38**, 10 (1984).
5. M. S. Webster, P. P. Marra, S. M. Haig, S. Bensch, R. T. Holmes, *Trends Ecol. Evol.* **17**, 76 (2002).
6. C. P. Chamberlain *et al.*, *Oecologia* **109**, 132 (1997).
7. K. A. Hobson, L. I. Wassenaar, *Oecologia* **109**, 142 (1997).
8. L. I. Wassenaar, K. A. Hobson, *Ecol. Appl.* **10**, 911 (2000).
9. C. P. Chamberlain, S. Bensch, X. Feng, S. Akesson, T. Andersson, *Proc. R. Soc. London Ser. B* **267**, 43 (2000).
10. K. A. Hobson, K. P. McFarland, L. I. Wassenaar, C. C. Rimmer, J. E. Goetz, *Auk* **118**, 16 (2001).
11. K. A. Hobson, L. I. Wassenaar, *Ecol. Appl.* **11**, 1545 (2001).
12. R. T. Holmes, in *The Birds of North America*, No. 87, A. Poole, F. Gill, Eds. (Academy of Natural Sciences, Philadelphia, PA, and The American Ornithologists' Union, Washington, DC, 1994).
13. H. Mizutani, M. Fukuda, Y. Kabaya, E. Wada, *Auk* **107**, 400 (1990).
14. A. B. Cormie, H. P. Schwartz, J. Gray, *Geochim. Cosmochim. Acta* **58**, 365 (1994).
15.  $\delta^{13}C$  values vary in plant tissue because of isotopic fractionation in the different photosynthetic pathways of  $C_3$ ,  $C_4$ , and Crassulacean acid metabolism plants (26, 27), as well as because of temperature differences that limit enzymatic reactions during photosynthesis and affect water use efficiency (27). These processes contribute to latitudinal and altitudinal trends in  $\delta^{13}C$  values in plant tissues (28, 29) and ultimately in animal tissues because of the input of this fractionated carbon from plants into the food web (14). In temperate North America,  $\delta^{13}C$  values tend to decrease with increasing

- latitude (6) and increase with increasing altitude (29).  $\delta D$  values in precipitation and surface waters [and ultimately in plant and animal tissues (14)] vary as a function of latitude, altitude, season, and distance inland (30, 31).  $\delta D$  values tend to decrease with increasing latitude in a northwesterly direction across North America (6–8, 14) and decrease with increasing altitude (30, 31).
16. Isotopic ratios ( $R$ ) of carbon and hydrogen are reported in  $\delta$  units:  $\delta = [(R_{\text{sample}}/R_{\text{standard}}) - 1] \times 1000$ .  $\delta^{13}C \pm 0.22$  per mil (‰), reported as the ratio of  $^{13}C/^{12}C$ ‰ relative to the Pee Dee belemnite standard, was analyzed with online analytical techniques (9). Mesquite plant standards of known isotopic composition (9) were used to systematically correct all of the online feather values to previously published offline values (6).  $\delta D \pm 5$ ‰, reported as the ratio of  $^2H/^1H$ ‰ relative to the Vienna standard mean ocean water standard, of wintering ground samples was analyzed with online analytical techniques (32). All of the feathers analyzed online for  $\delta D$  had remained at one location (Dartmouth College, NH) for at least 4 years and were analyzed over a 5-day period to minimize possible exchange with ambient water vapor. Breeding ground  $\delta D$  values were taken from previously reported values run with offline analytical techniques [exchangeable hydrogen was standardized before analysis by means of a high-temperature preparative equilibrium technique (6)]. We analyzed 15 feathers both offline and online.  $\delta D$  values did not significantly differ between the techniques ( $t_{15} = 0.77$ ,  $P = 0.46$ ), so no systematic correction was needed to compare the data sets.
17. The black-throated blue warbler is suitable as a study species because its breeding range covers a wide north-south gradient of  $\sim 17^\circ$  latitude, as well as a wide east-west gradient of  $\sim 26^\circ$  longitude across the northern portion of the breeding range (Fig. 1). It is mainly restricted to continuous tracts of undisturbed deciduous or mixed deciduous/coniferous forest habitat on mountainous slopes or at high elevation, where it feeds primarily on arthropods gleaned from foliage (12). Because the black-throated blue warbler is restricted almost exclusively to forested habitat,  $\delta^{13}C$  in its feathers is not complicated by  $C_4$  crops in agricultural fields (8).
18. Breeding ground samples consisted of flank feathers (nine sites) and tail feathers (one site), usually the third rectrix, from juvenile ( $<1$  year) and adult ( $>1$  year) male birds. There was no significant difference in  $\delta^{13}C$  between flank and tail feathers from within birds ( $t_{27} = 1.36$ ,  $P = 0.19$ ). Feather samples from NC were not analyzed for  $\delta D$ , and different samples from NH were analyzed for  $\delta^{13}C$  and  $\delta D$ , so samples from these sites could not be used in the regression models (20, 21). Samples from 8 of 10 breeding sites were collected within a single year (during 1989–1998), whereas birds from WV were sampled over 2 years and those from NH over 6 years. Although only male feather samples were used in all of the breeding ground analyses, we also examined a group of females from NH. With one exception, there were no significant effects of age, sex (NH only), or year, or their interactions, on  $\delta^{13}C$  (WV:  $F_{1,29} < 3.72$ ,  $P > 0.05$ ; NH:  $F < 1.76$ ,  $P > 0.05$ ,  $df = 1$  to 5 and 58); a significant effect of year for  $\delta^{13}C$  in NH ( $F_{5,59} = 4.64$ ,  $P = 0.002$ ) was due to high values in 1 of 6 years (mean  $\pm$  SE =  $-23.2 \pm 0.34$  in 1994 versus means of  $-24.4$  to  $-24.9$  for all other years). Wintering ground samples consisted of single tail feathers, usually the third rectrix, from juveniles ( $<10$  year) and adults ( $>1$  year) of both sexes. Samples from two of the Jamaica sites were not analyzed for  $\delta D$ . Each of the wintering sites was sampled in multiple years (1989–1997), and years did not differ in isotope ratios ( $\delta^{13}C$ :  $F_{20,349} = 1.55$ ,  $P > 0.05$ ;  $\delta D$ :  $F_{12,123} = 0.58$ ,  $P > 0.05$ ; year nested within site).
19. Breeding sites sampled in the southern portion of the breeding range tended to be at higher elevation than those in the north ( $F_{1,8} = 23.74$ ,  $P = 0.0012$ ,  $r^2 = 0.75$ ). Although  $\delta^{13}C$  tends to increase (28, 29) and  $\delta D$  tends to decrease (30, 31) with increasing altitude, the patterns we observed in feathers were due mainly to differences in the latitude of the sampling sites and not in the altitude at which the birds were captured ( $\delta^{13}C$ : latitude,  $F_{1,266} = 14.62$ ,  $P = 0.0002$ ; altitude,  $F_{1,266} = 2.57$ ,  $P = 0.11$ ; interaction,  $F_{1,266} = 2.33$ ,  $P = 0.13$ .  $\delta D$ :

- latitude,  $F_{1,129} = 7.33$ ,  $P = 0.0077$ ; altitude,  $F_{1,129} = 2.62$ ,  $P = 0.11$ ; interaction,  $F_{1,129} = 2.38$ ,  $P = 0.13$ ). Furthermore, we sampled birds from over 500 m of elevation at the NC site and found no effect of altitude on  $\delta^{13}C$  ( $F_{1,28} = 0.57$ ,  $P = 0.46$ ,  $r^2 = 0.02$ ).
20. We fit a regression model using both isotopes as independent variables. Breeding latitude =  $-12.55 - 1.95(\delta^{13}C) - 0.097(\delta D)$  ( $R^2 = 0.44$ ,  $n = 129$ ,  $P < 0.0001$  for both  $\delta^{13}C$  and  $\delta D$ ). The model correctly predicted breeding latitude to  $\pm 3.18^\circ$  (MSE $^{0.5}$ ).
21. We fit a regression model matching that in (20) but predicting breeding longitude instead of latitude. Breeding longitude =  $115.51 + 2.62(\delta^{13}C) - 0.28(\delta D)$  ( $R^2 = 0.34$ ,  $n = 69$ ,  $P = 0.017$  and  $P < 0.0001$  for  $\delta^{13}C$  and  $\delta D$ , respectively). The model correctly predicted breeding longitude to  $\pm 6.40^\circ$  (MSE $^{0.5}$ ).
22. R. Greenberg, in *Migrant Birds in the Neotropics*, A. Keast, E. S. Morton, Eds. (Smithsonian Institution Press, Washington, DC, 1980), pp. 593–604.
23. B. B. DeWolfe, L. F. Baptista, *Condor* **97**, 376 (1995).
24. M. A. Ramos, D. W. Warner, in *Migrant Birds in the Neotropics*, A. Keast, E. S. Morton, Eds. (Smithsonian Institution Press, Washington, DC, 1980), pp. 173–180.
25. R. Pellek, *J. Forest.* **88**, 15 (1990).
26. K. Lajtha, J. D. Marshall, in *Stable Isotopes in Ecolog-*

- ical and Environmental Sciences*, K. Lajtha, R. H. Michener, Eds. (Oxford Univ. Press, London, 1994), pp. 1–21.
27. B. N. Smith, S. Epstein, *Plant Physiol.* **47**, 380 (1971).
28. C. Korner, G. D. Farquhar, S. C. Wong, *Oecologia* **88**, 30 (1991).
29. K. R. Hultine, J. D. Marshall, *Oecologia* **123**, 32 (2000).
30. W. Dansgaard, *Tellus* **16**, 436 (1964).
31. H. Ziegler, in *Stable Isotopes in Ecological Research*, P. W. Rundel, J. R. Ehleringer, K. A. Nagy, Eds. (Springer-Verlag, New York, 1988), pp. 105–123.
32. Z. D. Sharp, V. Atudorei, T. Durakiewicz, *Chem. Geol.* **178**, 197 (2000).
33. Supported by undergraduate research grants from Dartmouth College, the Howard Hughes Medical Institute, and the Andrew W. Mellon Foundation to D.R.R., as well as research grants from NSF to R.T.H. and C.P.C. and from the Smithsonian Institution to G.R.G. S. Latta, G. Wallace, and J. Wunderle provided feather samples from Hispaniola, Cuba, and Puerto Rico, respectively. X. Feng and M. Poage helped with the isotopic analyses. We thank S. Emlen, P. Marra, D. I. Rubenstein, P. Sherman, S. Sillett, and M. Wikelski for constructive comments.

15 October 2001; accepted 7 December 2001

## Melanopsin-Containing Retinal Ganglion Cells: Architecture, Projections, and Intrinsic Photosensitivity

S. Hattar,<sup>1,2\*</sup> H.-W. Liao,<sup>2\*</sup> M. Takao,<sup>4</sup> D. M. Berson,<sup>4</sup> K.-W. Yau<sup>1,2,3†</sup>

The primary circadian pacemaker, in the suprachiasmatic nucleus (SCN) of the mammalian brain, is photoentrained by light signals from the eyes through the retinohypothalamic tract. Retinal rod and cone cells are not required for photoentrainment. Recent evidence suggests that the entraining photoreceptors are retinal ganglion cells (RGCs) that project to the SCN. The visual pigment for this photoreceptor may be melanopsin, an opsin-like protein whose coding messenger RNA is found in a subset of mammalian RGCs. By cloning rat melanopsin and generating specific antibodies, we show that melanopsin is present in cell bodies, dendrites, and proximal axonal segments of a subset of rat RGCs. In mice heterozygous for tau-lacZ targeted to the melanopsin gene locus,  $\beta$ -galactosidase-positive RGC axons projected to the SCN and other brain nuclei involved in circadian photoentrainment or the pupillary light reflex. Rat RGCs that exhibited intrinsic photosensitivity invariably expressed melanopsin. Hence, melanopsin is most likely the visual pigment of phototransducing RGCs that set the circadian clock and initiate other non-image-forming visual functions.

Retinal rods and cones, with their light-sensitive, opsin-based pigments, are the primary photoreceptors for vertebrate vision. Visual sig-

nals are transmitted to the brain through RGCs, the output neurons whose axons form the optic nerve. This system, through its projections to the lateral geniculate nucleus and the midbrain, is responsible for interpreting and tracking visual objects and patterns. A separate visual circuit, running in parallel with this image-forming visual system, encodes the general level of environmental illumination and drives certain photic responses, including synchronization of the biological clock with the light-dark cycle (1), control of pupil size (2), acute sup-

<sup>1</sup>Howard Hughes Medical Institute and Departments of <sup>2</sup>Neuroscience and <sup>3</sup>Ophthalmology, Johns Hopkins University School of Medicine, 725 North Wolfe Street, Baltimore, MD 21205–2185, USA. <sup>4</sup>Department of Neuroscience, Brown University, Providence, RI 02912, USA.

\*These authors contributed equally to this work.  
†To whom correspondence should be addressed. E-mail: kwyau@mail.jhmi.edu